Article:
Caseley, EA orcid.org/0000-0001-7591-143X, Muench, SP orcid.org/0000-0001-6869-4414 and Jiang, L-H orcid.org/0000-0001-6398-0411 (2022) Tyrosine 288 in the extracellular domain of the human P2X7 receptor is critical for receptor function revealed by structural modeling and site-directed mutagenesis. Proteins: Structure, Function, and Bioinformatics, 90 (3). pp. 619-624. ISSN 0887-3585

https://doi.org/10.1002/prot.26259

Tyrosine 288 in the extracellular domain of the human P2X7 receptor is critical for receptor function revealed by structural modelling and site-directed mutagenesis

Emily A Caseley [1, 2,*], Stephen P Muench [2] and Lin-Hua Jiang [2, *]

[1]Leeds Institute of Rheumatic and Musculoskeletal Medicine, St James's University Hospital, and [2]School of Biomedical Sciences, Faculty of Biological Sciences, University of Leeds

*Correspondence: Dr Emily A Caseley (e.a.caseley@leeds.ac.uk) or Dr Lin-Hua Jiang (l.h.jiang@leeds.ac.uk; Tel.: +44 113 3434231).

Abstract

The P2X7 receptor (P2X7R) is a calcium-permeable cation channel activated by high concentrations of extracellular ATP. It plays a role in vital physiological processes, particularly in innate immunity, and is dysregulated in pathological conditions such as inflammatory diseases, neurodegenerative diseases, mood disorders and cancers. Structural modelling of the human P2X7R (hP2X7R) based on the recently available structures of the rat P2X7 receptor (rP2XR) in conjunction with molecular docking predicts the orientation of tyrosine at position 288 (Y288) in the extracellular domain to face ATP. In this short communication, we combined site-directed mutagenesis and whole-cell patch clamp recording to investigate the role of this residue in the hP2X7R function. Mutation of this extracellular residue to amino acids with different properties massively impaired current responses to both ATP and BzATP, suggesting that Y288 is important for normal receptor function. Such a finding facilitates development of an in-depth understanding of the molecular basis of hP2X7R structure-function relationships.

Keywords: P2X7R; structure-function relationships; structural modelling; molecular docking; site-directed mutagenesis; patch-clamp recording

Introduction

Extracellular adenosine triphosphate (ATP) acts as a signalling molecule that evokes purinergic signalling through purinergic receptors, including P2X receptors (P2XRs), a group of trimeric, ligand-gated ion channels made of seven subunits (P2X1-7). The P2X7 receptor (P2X7R) is distinct from the other P2XRs in part due to its relative insensitivity to ATP, requiring sub-millimolar to millimolar concentrations compared to submicromolar concentrations for other P2XRs, and its higher sensitivity to the synthetic ATP analogue benzoylbenzoyl-ATP (BzATP) than ATP (Surprenant et al., 1996; Rassendren et al., 1997). The P2X7R is highly expressed in immune cells, particularly macrophages and microglia, where it has an integral function in regulating innate immune responses, and alteration in its expression and/function is strongly implicated in inflammation in the pathogenesis of clinical

conditions such as chronic pain, neurodegenerative diseases and mood disorders (e.g., Adinolfi et al., 2018; Bhattacharya and Jones, 2018; Wei et al., 2018; Andrejew et al., 2020; Jiang and Roger, 2020; Pelegrin, 2021; Engel et al., 2021). The hP2X7R thus remains an attractive pharmacological target (e.g., Cao et al., 2019; Koch-Nolte et al., 2019; Illes et al., 2019; Calzaferri et al., 2020; Territo and Zarrinmayeh, 2021). As such, understanding amino acid residues that can influence the function of the hP2X7R is a subject of much scrutiny. Indeed, numerous residues in the P2X7R have been identified as important determinants for its function, by influencing different functional aspects of the P2X7R (Jiang et al., 2013, 2021). This short communication reports Y288 in the hP2X7R to be critical for its normal function.

Materials and Methods

Homology modelling Structural models of the hP2X7R were generated based on the cryo-electron microscopy structures of the rP2X7R in closed and ATP-bound open states (Protein Data Bank code 6U9V and 6U9W, respectively). Models were produced in Modeller version 9.12 (Webb and Sali, 2006) and subsequently analysed in MolProbity (Davis et al., 2007) as detailed in our previous studies (Caseley et al., 2015, 2016, 2020).

Molecular docking Docking studies were carried out in AutoDock version 4.2 (Morris et al., 2009) against a target cavity file consisting of a 15-Å sphere surrounding the ATP-binding site in the homology models generated above, with the bound ATP molecule used as the central point. Affinity grid files were generated using the auxiliary program AutoGrid. The ATP molecule bound within the binding site in the crystal structure was used as the centre of these grids. A model of the 2′ isomer of BzATP was used in docking.

Site-directed mutagenesis cDNA for the wildtype (WT) hP2X7 receptor tagged with a C-terminal EE (EYMPME) epitope was subcloned into a pcDNA3.1 vector as outlined in previous studies (Bradley et al., 2011). Site-directed mutagenesis was used to introduce point mutations as described (Yang and Jiang, 2013) and confirmed by commercial sequencing (Beckman Coulter Genomics).

Patch-clamp recording Human embryonic kidney (HEK) 293 cells were transiently transfected with WT or mutant hP2X7Rs using Lipofectamine 2000 (Invitrogen). Whole-cell currents were measured using patch-clamp recording. The EC_{50} values were derived by fitting the concentration-current response relationship curves to Hill equation, as detailed in previous studies (Bradley et al., 2011; Caseley et al., 2016).

Data analysis Results are presented as the mean ± standard error of the mean (SEM), where appropriate. Curve fits were carried out in Origin software. Student's t-test was used to compare two groups, and

one-way analysis of variance (ANOVA) test with Tukey's post-hoc test was used for more than two groups. A $p < 0.05$ was considered significant.

Results

Molecular docking was carried out to dock ATP and BzATP into the extracellular region of a homology model of the hP2X7R (Fig.1A) that was generated using the recently reported structures of the rP2X7R (McCarthy et al., 2019). ATP binding at the subunit interface is coordinated by a subset of highly conserved residues from two neighbouring subunits, including K64, K66, T189, N292, R294 and K311 in the hP2X7R structural model (left panel in Fig.1B) as described in the rP2X7R structure (right panel in Fig.1B). As illustrated by conformations of BzATP with the two lowest predicted binding energies docked to the hP2X7R structural model, many of these ATP-binding residues and additional highly conserved residues such as Q143, I214 and I228 are predicted to be engaged in BzATP binding to the hP2X7R (Fig.1C).

Interestingly, interrogating this region revealed that tyrosine at position 288 (Y288), in the hP2X7R, particularly its aromatic side chain, assumes an orientation facing towards ATP (Fig.1B). A previous study showed that introduction of Y288F mutation into the hP2X7R, which replaced Y288 with phenylalanine, the corresponding residue in the rP2X7R (Fig.1B), affected receptor deactivation (Ischchenko et al., 2017). However, it remained unclear whether this position influences agonist binding and/or conformal changes required for receptor activation.

We introduced point mutation of Y288 in the hP2X7R with residues with different side chain, serine, glycine, and valine (Y288S, Y288G, and Y288V) as well as phenylalanine (Y288F). We expressed the WT and mutant hP2X7R in HEK293 cells and assessed the mutational effects on the hP2X7R current response to a range of concentrations of the potent P2X7R agonist, BzATP (Fig.2), as well as the physiological agonist, ATP (Fig.3). Y288G, Y288S and Y288V mutations drastically impaired the current responses to BzATP at all concentrations (Fig.2A-B); the mean amplitude of maximal currents elicited by 300 μM BzATP was reduced from 4458 ± 580 pA from the WT hP2X7R to 120 ± 41, 115 ± 53 and 101 ± 22 pA, respectively (Fig.2C). Surprisingly, the maximal current amplitude for the hP2X7 receptor carrying the Y288F mutation, 274 ± 59 pA, although being approximately double of that seen in the other three mutants, was significantly lower than that from the WT hP2X7R. Similarly, mutation of Y288 decreased the current responses to ATP at all concentrations (Fig.3A-B). The mean maximal currents induced by 10 mM ATP were 75 ± 25, 115 ± 53 and 111 ± 24 pA for Y288G, Y288S and Y288V, respectively, markedly smaller than 4268 ± 640 pA from the WT hP2X7R. Similar to the current response to BzATP, the mean maximal current response of Y288F mutant receptor, 140 ± 101 pA, was slightly higher than that of other Tyr288 mutant receptors (Fig.3C).

It has been demonstrated that many individual residues in the P2X7R influence agonist sensitivity, including those disease-related ones arising from non-synonymous single nucleotide polymorphisms (NS-SNPs) in humans (Young et al., 2007; Jiang et al., 2013). We thus further

determined the EC_{50} values of the WT and mutant hP2X7Rs in order to examine the mutational effects on the sensitivity of the hP2X7R to BzATP and ATP. Despite significantly reduced current responses, the BzATP EC_{50} value for the Y288V and Y288F mutant receptors was comparable to that of the WT hP2X7R, whereas the BzATP EC_{50} value for the Y288G and Y288S mutant receptors was considerably reduced (Fig.2D). In contrast, the Y288V and Y288F mutant receptors exhibited a significantly higher EC_{50} value in response to ATP, whereas the Y288G and Y288S mutant receptors had an EC_{50} value comparable to that of the WT hP2X7R (Fig.3D). Collectively, these results indicate that these mutations also affect agonist sensitivity as well as agonist-induced current responses at the hP2X7R.

Discussion

Many residues in various parts of the hP2X7R play an important role in receptor function, as demonstrated by naturally occurring or engineered mutations that affect channel function (Young et al., 2007; Roger et al., 2010; Bradley et al., 2011; Caseley et al., 2014, 2020). Here, we combined structural modelling, based on the recently reported structures of the rP2X7R, and molecular docking to identify residues in the extracellular domain proximal to the highly conserved ATP-binding site in the hP2X7R, revealing Y288 as being of interest for its close position to ATP, particularly its ATP-facing orientation (Fig.1B). Our results show that substitution of Y288 with residues with side chains of varying properties led to a drastic loss of the current responses to both ATP and BzATP (Fig.2 and Fig.3). Surprisingly, even replacement of Y288 with the corresponding residue F288 in the rP2X7 receptor massively impaired the current responses to ATP and BzATP. Collectively, these results suggest that Y288 is critically required for normal function of the hP2X7R.

The location of residue 288 can be examined thanks to the recent determination of the full-length rP2X7R structure (McCarthy et al., 2019), which facilitates the production of hP2X7R homology models (Fig.1A). Previous studies utilising similar molecular docking approaches have also identified several conserved residues as important in coordinating BzATP binding, including Q143, T189 and I228 (Dal Ben et al., 2015; Pasqualetto et al., 2018). Similar results were obtained in this study (Fig.1C). Furthermore, Dal Ben et al (2015) proposed that hindrance of Y/F288 affected agonist-P2X7R interactions, a notion that is overall supported by our results from site-directed mutagenesis. In the rP2X7R structure, F288 in the extracellular domain occupies a position proximal to L191, I214 and I228, which together form a hydrophobic milieu that influences interactions of ATP, particularly the ribose and adenine, with the ATP-binding site (right panel in Fig.1B). In addition, F288 forms the bottom half of the ATP 'jaw' that tightens following ATP binding to activate the rP2X7R (Jiang et al., 2021). Change to Y288 in the hP2X7R with a different orientation may influence the interaction with agonist and/or the conformational changes required for receptor activation. A recent study has reported that introduction of the Y288S mutation in a human P2X7 receptor, in which residues 16-26 in the intracellular N-terminus was replaced by the corresponding region of the hP2X2 receptor, significantly reduced both ATP-induced maximal current response and the EC_{50} for ATP (Allsopp et al., 2017).

These results are overall consistent with our results (Fig.3), though the mutational effects were less prominent than what we observed. Our previous study reported NS-SNP mutations H155Y, also located in the extracellular domain, impaired normal hP2X7R function by altering cell surface expression (Bradley et al., 2011). Our preliminary results using immuno-fluorescent confocal microscopy suggest that mutation of Y288 may also negatively affect the cell surface expression (Supplementary Fig.1) that may in part contribute to loss of receptor function. The residue 288 is located however far away from the transmembrane ion-conducting pore, suggesting that mutating F288 unlikely altered the function of the ion-permeating pathway.

In summary, this study reports Tyr288 in the extracellular domain of the hP2X7R as an important molecular determinant for receptor activation, cell surface expression or both.

Author Contributions

Conceptualization: L-HJ, EAC and SPM; data acquisition and analysis: EAC; writing-original draft preparation: EAC; writing-review and editing: L-HJ and SPM. All authors have read and agreed to the published version of the manuscript.

Acknowledgments

We are grateful to Mrs Jocelyn Baldwin for the instructions of homology modelling. The project was supported by the Wellcome Trust (099758/Z/12/Z).

Conflicts of Interest

The authors declare no conflict of interest.

Figure legends

Fig. 1 Location of Y288 in the hP2X7R ATP-binding site. (A) Homology model of the trimeric hP2X7R in the closed state composed of extracellular, transmembrane and intracellular and domains, based on the rP2X7R structure (PDB 6U9V). The location of residue Y288 at one subunit interface is illustrated in yellow spheres. (B) Close-up view showing the relative position of residue Y288 in yellow to key residues coordinating the binding for the ATP molecule docked to the hP2X7R structure model (left) and in the rP2X7R structure (right). (C) Conformations of BzATP with the two lowest predicted binding energies docked to the structural model of the hP2X7R in ATP-bound state, showing residues predicted to coordinate BzATP binding.

Fig. 2 Impact of mutating hP2X7R residue Y288 on BzATP-induced currents. (A) Representative current responses evoked by BzATP at concentrations indicated from HEK293 cells transiently expressing the WT or mutant hP2X7R. (B) Concentration-current response relationship curves from

recordings shown in A; solid lines represent data fit to the Hill equation. (C) Summary of the maximal currents evoked by 300 μM BzATP, and BzATP EC_{50} values. ** $p < 0.01$ compared to WT.

Fig. 3 Impact of mutating hP2X7R residue Y288 on ATP-induced currents. (A) Representative current responses evoked by ATP at concentrations indicated from HEK293 cells transiently expressing the WT or mutant hP2X7R. (B) Concentration-current response relationship curves from recordings shown in A; solid lines represent data fit to the Hill equation. (C) Summary of the maximal current evoked by 10 mM ATP, and ATP EC_{50} values. ** $p < 0.01$ compared to WT.

References

Adinolfi E, Giuliani AL, De Marchi E, Pegoraro A, Orioli E and Di Virgilio F (2018) The P2X7 receptor: A main player in inflammation. *Biochem Pharmacol* **151**:234-244.

Andrejew R, Oliveira-Giacomelli Á, Ribeiro DE, Glaser T, Arnaud-Sampaio VF, Lameu C and Ulrich H. (2020) The P2X7 receptor: Central hub of brain diseases. *Front Mol Neurosci* **13**:124.

Allsopp RC, Dayl S, Schmid R and Evans RJ (2017) Unique residues in the ATP gated human P2X7 receptor define a novel allosteric binding pocket for the selective antagonist AZ10606120. Sci Rep **7**:725.

Bhattacharya A and Jones DN (2018) Emerging role of the P2X7-NLRP3-IL1β pathway in mood disorders. *Psychoneuroendocrinology* **98**:95-100.

Bradley H J, Baldwin JM, Goli GR, Johnson B, Zou J. Sivaprasadarao A, Baldwin SA and Jiang L-H (2011) Residues 155 and 348 contribute to the determination of P2X7 receptor function via distinct mechanisms revealed by single-nucleotide polymorphisms. *J Biol Chem* **286**:8176-8187.

Calzaferri F, Ruiz-Ruiz C, de Diego AMG, de Pascual R, Méndez-López I, Cano-Abad MF, Maneu V, de Los Ríos C, Gandía L and García AG (2020) The purinergic P2X7 receptor as a potential drug target to combat neuroinflammation in neurodegenerative diseases. *Med Res Rev* **40**:2427-2465.

Cao F, Hu LQ, Yao SR, Hu Y, Wang DG, Fan YG, Pan GX, Tao SS, Zhang Q, Pan HF and Wu GC (2019) P2X7 receptor: A potential therapeutic target for autoimmune diseases. *Autoimmun Rev* **18**:767-777.

Caseley EA, Muench SP, Roger S, Mao HJ, Baldwin SA and Jiang LH (2014) Non-synonymous single nucleotide polymorphisms in the P2X receptor genes: association with diseases, impact on receptor functions and potential use as diagnosis biomarkers. *Int J Mol Sci* **15**:13344-13371.

Caseley EA, Muench SP, Baldwin SA, Simmons K, Fishwick CW and Jiang LH (2015) Docking of competitive inhibitors to the P2X7 receptor family reveals key differences responsible for changes in response between rat and human. *Bioorg Med Chem Lett* **25**:3164-3167.

Caseley EA, Muench SP, Fishwick CW and Jiang L-H (2016) Structure-based identification and characterisation of structurally novel human P2X7 receptor antagonists. *Biochem Pharmacol* **116**:130-139.

Caseley EA, Muench SP and Jiang L-H (2020) Contribution of Val/Ile87 residue in the extracellular domain in agonist-induced current responses of the human and rat P2X7 receptors. *Purinergic Signal* **16**:485-490.

Dal Ben D, Buccioni M, Lambertucci C, Marucci G, Thomas A and Volpini R (2015) Purinergic P2X receptors: structural models and analysis of ligand-target interaction. *Euro J Med Chem* **89**:561-580.

Davis IW, Leaver-Fay A, Chen VB, Block JN, Kapral GJ, Wang X, Murray LW, Arendall WB 3rd, Snoeyink J, Richardson JS and Richardson DC (2007) MolProbity: all-atom contacts and structure validation for proteins and nucleic acids. *Nucleic Acids Res* **35**: W375-W383.

Engel T, Nicke A, Deussing JM, Sperlagh B and Diaz-Hernandez M. (2021) Editorial: P2X7 as common therapeutic target in brain diseases. *Front Mol Neurosci* **14**:656011.

Illes P, Rubini P, Huang L and Tang Y (2019) The P2X7 receptor: a new therapeutic target in Alzheimer's disease. *Expert Opin Ther Targets* **23**:165-176.

Ishchenko Y, Novosolova N, Khafizov K, Bart GV, Timonina A, Fayuk D, Skorinkin A, Giniatullin R (2017) Reconstructed serine 288 in the left flipper region of the rat P2X7 receptor stabilizes nonsensitized states. *Biochemistry* **56**:3394-3402.

Jiang L-H, Baldwin JM, Roger S and Baldwin SA (2013) Insights into the molecular mechanisms underlying mammalian P2X7 receptor functions and contributions in diseases, revealed by structural modeling and single nucleotide polymorphisms. *Front Pharmacol* **4**:55.

Jiang LH and Roger S (2020) Targeting the P2X7 receptor in microglial cells to prevent brain inflammation. *Neural Regen Res* **15**:1245-1246.

Jiang L-H, Caseley EA, Muench SP and Roger S (2021) Structural basis for the functional properties of the P2X7 receptor for extracellular ATP receptors. *Purinergic Signal* doi: 10.1007/s11302-021-09790-x

Koch-Nolte F, Eichhoff A, Pinto-Espinoza C, Schwarz N, Schäfer T, Menzel S, Haag F, Demeules M, Gondé H and Adriouch S (2019) Novel biologics targeting the P2X7 ion channel. *Curr Opin Pharmacol* **47**:110-118.

McCarthy AE, Yoshioka C and Mansoor SE (2019) Full-Length P2X7 structures reveal how palmitoylation prevents channel desensitization. *Cell* **179**:659-670.

Morris GM, Huey R, Lindstrom W, Sanner MF, Belew RK, Goodsell DS and Olson AJ (2009) AutoDock4 and AutoDockTools4: Automated docking with selective receptor flexibility. *J Comp Chem* **30**: 2785-2791

Pasqualetto G, Brancale A and Young MT (2018) The molecular determinants of small-molecule ligand binding at P2X receptors. *Front Pharmacol* **9**:58.

Pelegrin P (2021) P2X7 receptor and the NLRP3 inflammasome: Partners in crime. *Biochem Pharmacol* **187**:114385.

Rassendren F, Buell GN, Virginio C, Collo G, North RA and Surprenant A (1997) The permeabilizing ATP receptor, P2X7 cloning and expression of a human cDNA. *J Biol Chem* **272**:5482-5486.

Roger S, Mei ZZ, Baldwin JM, Dong L, Bradley H, Baldwin SA, Surprenant A and Jiang LH (2010) Single nucleotide polymorphisms that were identified in affective mood disorders affect ATP-activated P2X7 receptor functions. *J Psychiatr Res* **44**:347-355

Surprenant A, Rassendren F, Kawashima E, North RA and Buel, G (1996) The cytolytic P2Z receptor for extracellular ATP identified as a P2X receptor (P2X7). *Science* **272**:735-738.

Territo PR and Zarrinmayeh H (2021) P2X7 receptors in neurodegeneration: Potential therapeutic applications from basic to clinical approaches. *Front Cell Neurosci* **15**:617036.

Webb B and Sali A (2016) Comparative protein structure modeling using MODELLER. *Curr Protoc Protein Sci* **54**: 5.6.1-5.6.37.

Wei L, Syed Mortadza SA, Yan J, Zhang L, Wang L, Yin Y, Li C, Chalon S, Emond P, Belzung C, Li D, Lu C, Roger S and Jiang LH (2018) ATP-activated P2X7 receptor in the pathophysiology of mood disorders and as an emerging target for the development of novel antidepressant therapeutics. *Neurosci Biobehav Rev* **87**:192-205.

Yang W and Jiang L-H (2013) Site-directed mutagenesis to study the structure–function relationships of ion channels. *Methods Mol Biol* **998**:257-266.

Young MT, Pelegrin P and Surprenant A (2007) Amino acid residues in the P2X7 receptor that mediate differential sensitivity to ATP and BzATP. *Mol Pharmacol* **71**:92-100.

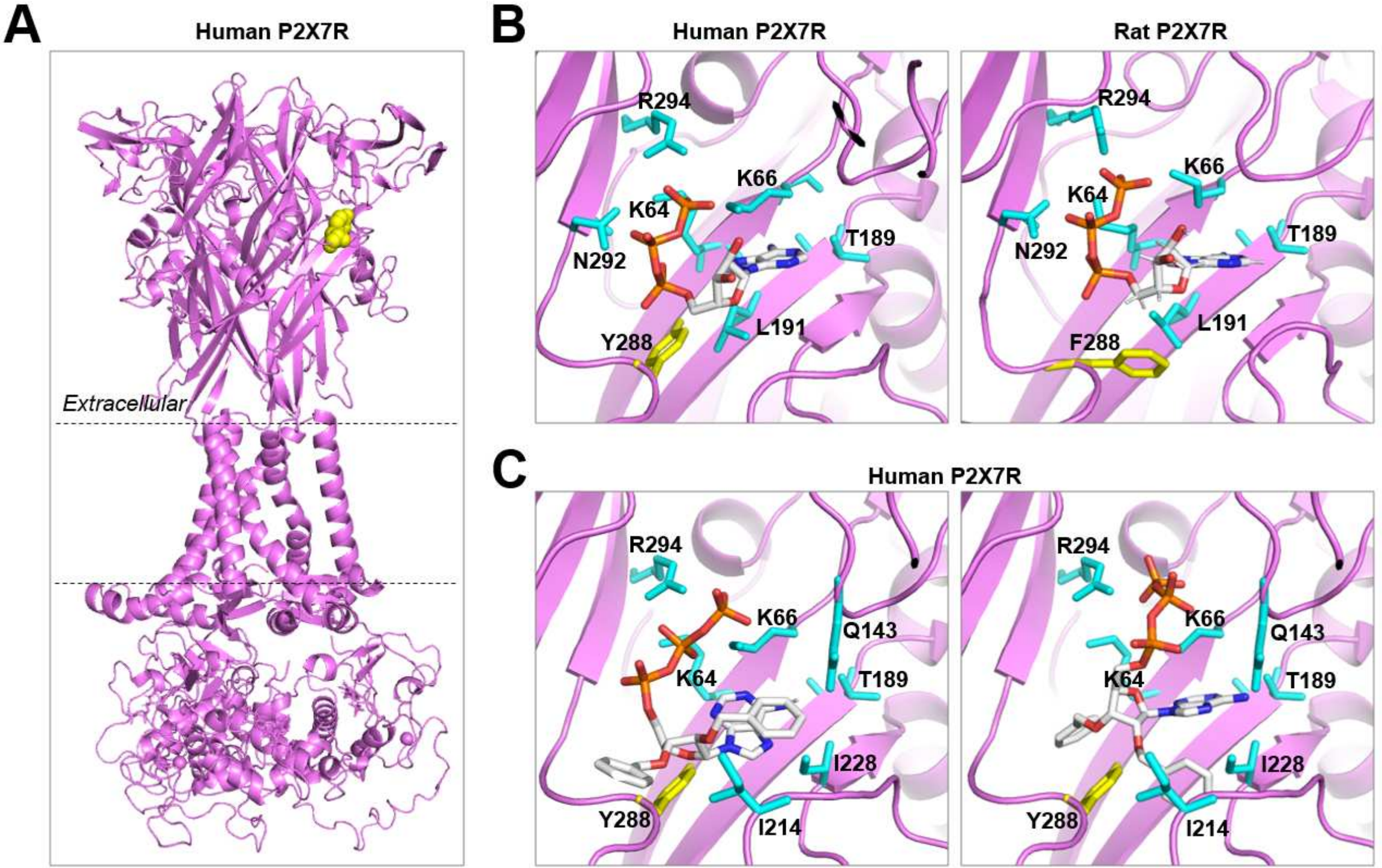
A
Human P2X7R
Extracellular
B
Human P2X7R
R294
K66
K64
N292
T189
L191
Y288
Rat P2X7R
R294
K66
K64
N292
T189
L191
F288
C
Human P2X7R
R294
K66
Q143
K64
T189
I228
Y288
I214
R294
K66
Q143
K64
T189
I228
Y288
I214

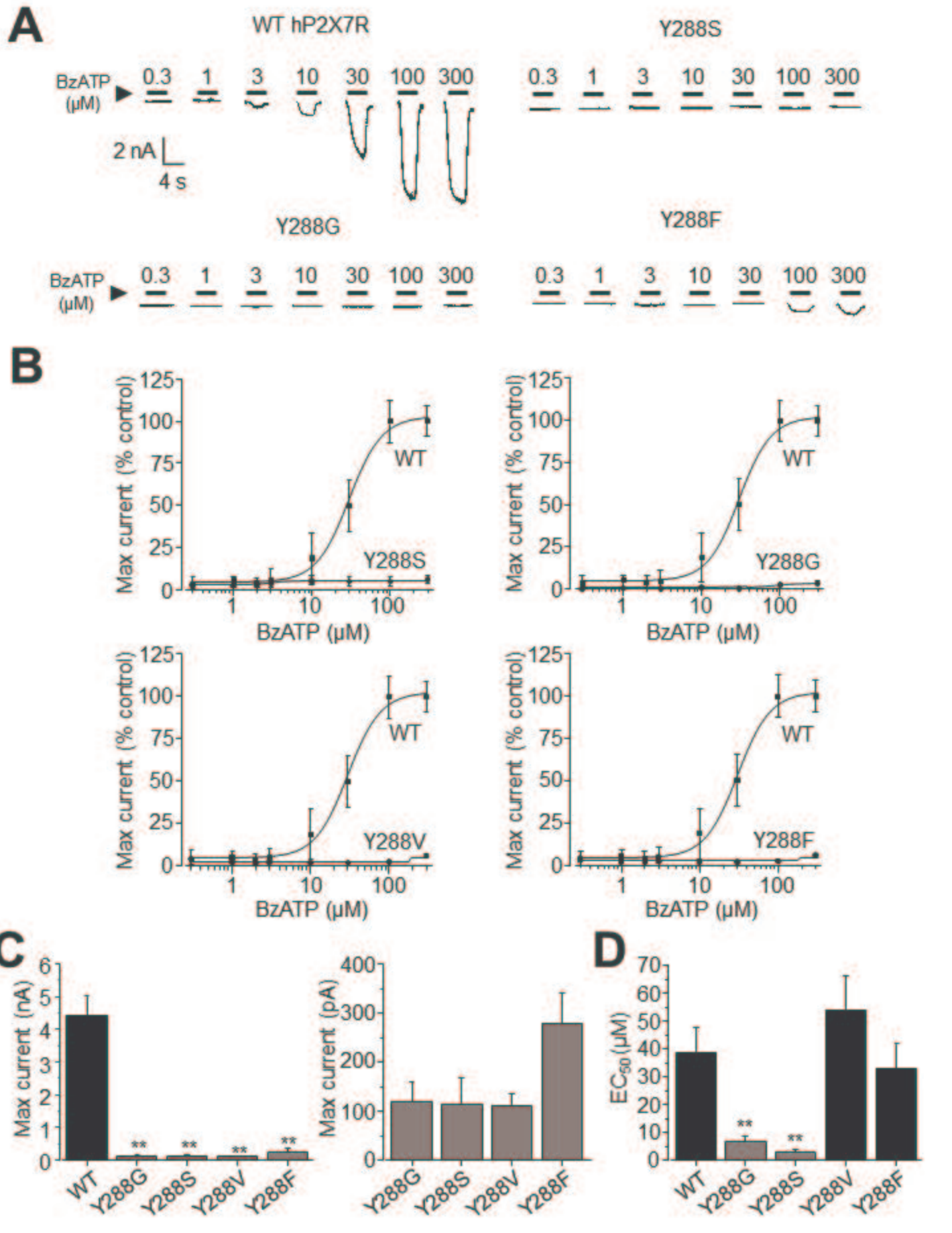
A
WT hP2X7R
Y288S
BzATP (μM)
0.3
1
3
10
30
100
300
2 nA
4 s
Y288G
Y288F
B
Max current (% control)
WT
Y288S
Y288G
Y288V
Y288F
BzATP (μM)
C
Max current (nA)
Max current (pA)
WT
Y288G
Y288S
Y288V
Y288F
D
EC50 (μM)

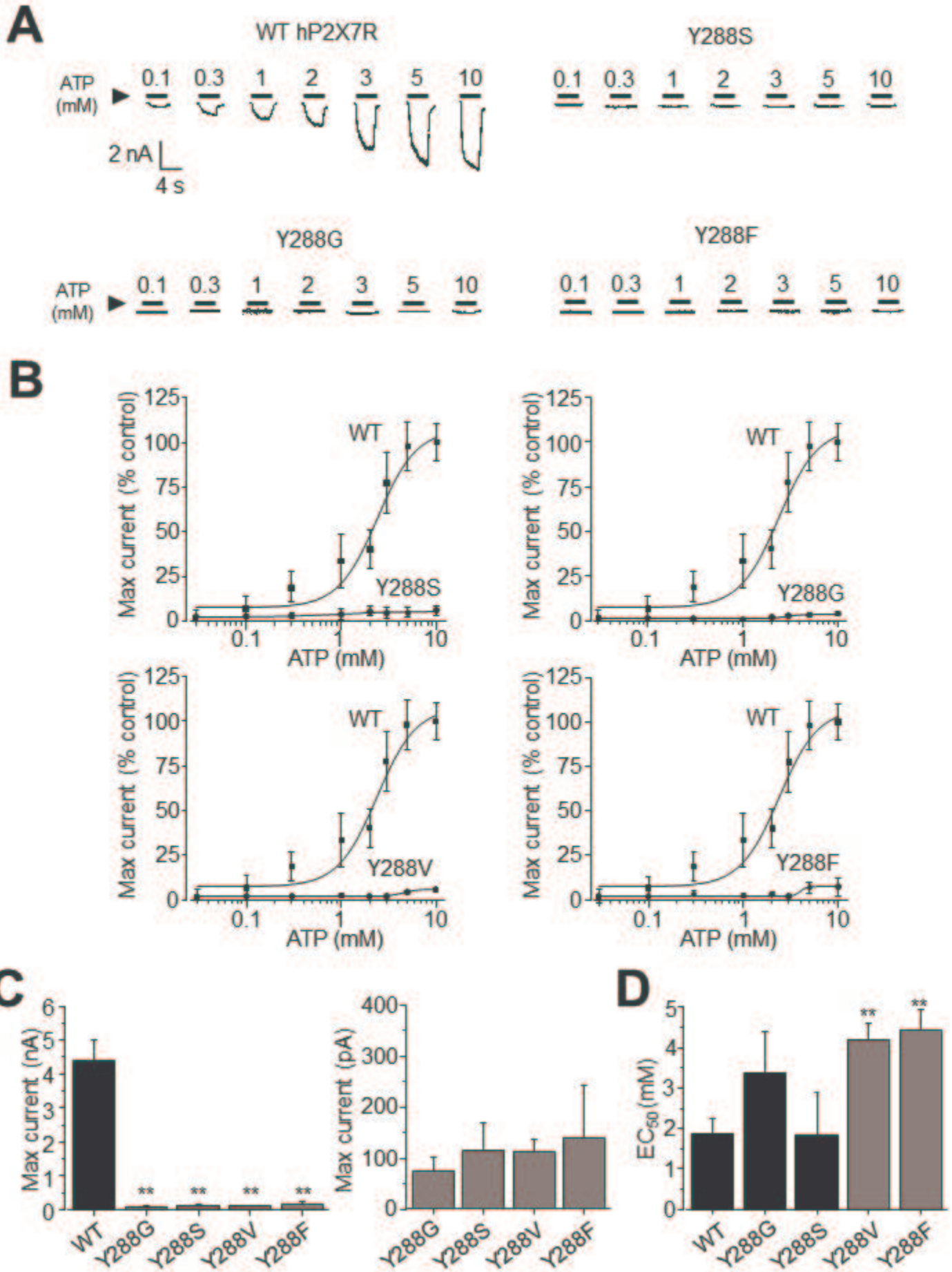
A
WT hP2X7R
Y288S
ATP (mM)
0.1 0.3 1 2 3 5 10
2 nA
4 s
Y288G
Y288F
B
Max current (% control)
WT
Y288S
Y288G
Y288V
Y288F
ATP (mM)
C
Max current (nA)
Max current (pA)
WT
Y288G
Y288S
Y288V
Y288F
D
EC50 (mM)
**